Macromolecular Research, Vol. 15, No. 5, pp 449-458 (2007)

Comparison of the Properties of Poly(butylene terephthalate) Nanocomposite Fibers with Different Organoclays

Jeong-Cheol Kim

Gwangju R&D Center, Korea Institute of Industrial Technology, Gwangju 500-460, Korea

Jin-Hae Chang*

Department of Polymer Science and Engineering, Kumoh National Institute of Technology, Gumi 730-701, Korea

Received April 2, 2007; Revised May 28, 2007

Abstract: The aims of this study were to investigate the intercalation of polymer chains with organoclays and improve the thermo-mechanical properties of poly(butylene terephthalate) (PBT) hybrids by comparing PBT hybrids synthesized using two different organoclays. The organoclays; dodecyltriphenylphosphonium-montmorillonite (C_{12}PPh-MMT) and dodecyltriphenylphosphonium-mica (C_{12}PPh-Mica), were used to fabricate the PBT hybrid fibers. Variations in the properties of the hybrid fibers with the organoclays within the polymer matrix, as well as the draw ratio (DR), are discussed. The thermo-mechanical properties and morphologies of the PBT hybrid fibers were characterized using differential scanning calorimetry, thermogravimetric analysis, wide-angle X-ray diffraction, electron microscopy and mechanical tensile properties analysis. The nanostructures of the hybrid fibers were determined using both scanning and transmission electron microscopies, which showed some of the clay layers to be well dispersed within the matrix polymer, although some clustered or agglomerated particles were also detected. The thermal properties of the hybrid fibers were found to be better than those of the pure PBT fibers at a DR = 1. The tensile mechanical properties of the C_{12}PPh-MMT hybrid fibers were found to worsen with increasing DR. However, the initial moduli of the C_{12}PPh-Mica hybrid fibers were found to slightly increase on increasing the DR from 1 to 18.

Keywords: poly(butylene terephthalate), nanocomposite, organoclay, fiber.

Introduction

Poly(butylene terephthalate) (PBT) is a typical semicrystalline polymer and is an important commercially available engineering thermoplastic for injection molding applications because of its excellent processability and flow properties. However, PBT has poor thermo-mechanical properties. Many attempts have been made to improve the properties of PBT by blending it with various fillers.[1-5]

Nanocomposites consist of ultrafine inorganic particles with sizes on the order of nanometers that are homogeneously dispersed in a polymer matrix. Nanocomposites possess properties that are superior to those of conventional composites because of their superior interfacial adhesion.[6-10]

Clay minerals contain alkali metals between silicate sheets and can swell in polar solvents such as water. There are many types of clays: kaolinite, montmorillonite, hectorite, saponite, synthetic mica, etc. Among them, montmorillonite (MMT) and mica have recently received significant attention as reinforcing materials for polymers owing to their high aspect ratio and unique characteristics. These clays consist of stacked silicate sheets with lengths of about 218 nm for montmorillonite and 1,230 nm for synthetic mica, and have the same sheet thickness, 1 nm.[11,12]

Several methods have been used to obtain nanocomposites of polymers with organoclays, specifically solution intercalation, melt intercalation, and *in situ* interlayer intercalation. In the *in situ* interlayer polymerization method,[13-16] the organoclay is swelled with the monomer, and then in situ polymerization is initiated either thermally or by the addition of a suitable compound. Chain growth in the clay galleries induces clay exfoliation and nanocomposite formation.

The objective of this study was to evaluate the effects of varying the amount of organoclay and the draw ratio on the properties of the PBT hybrid fibers. To obtain nanocomposites that do not undergo thermal degradation during processing, we used the thermally stable organoclays C_{12}PPh-MMT and C_{12}PPh-Mica. This paper examines the effects of the addition of these organoclays on the thermal behaviors, ten-

*Corresponding Author. E-mail: changjinhae@hanmail.net

sile mechanical properties, and morphologies of the hybrid fibers. The properties of the C_{12}PPh-MMT/PBT hybrid fibers were compared with those of fibers prepared from the C_{12}PPh-Mica/PBT hybrids.

Experimental

Materials. Source clay, Kunipia-F (Na^+-montmorillonite), was obtained from Kunimine Co. By screening this Na^+-montmorillonite (Na^+-MMT) clay with a 325-mesh sieve to remove impurities, we obtained a clay with a cationic exchange capacity of 119 meq/100 g. Na^+-type fluorinated synthetic mica (Na^+-Mica) with the free -OH group of the mica replaced by fluorine was supplied by CO-OP Ltd., Japan. Its cationic exchange capacity was found to be in the 70-80 meq/100 g range.

All reagents were purchased from TCI and Aldrich Chemical Co. Commercially available solvents were purified by distillation. Common reagents were used without further purification.

Preparation of Organoclays. Dispersions of Na^+-MMT and Na^+-Mica were added to solutions of the phosphonium salt of dodecyltriphenyl ($C_{12}PPh^-$). The two organophilic clays were obtained through a multi-step process with the same methods as described in our previous paper,[17] and are denoted C_{12}PPh-MMT and C_{12}PPh-Mica. The chemical structures of the C_{12}PPh-clays are as follows:

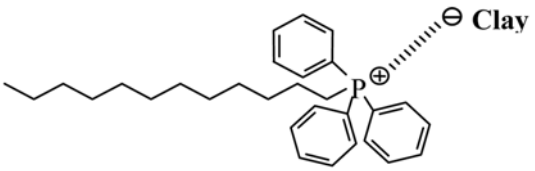

Preparation of PBT/Organoclay Hybrids. All of the samples were prepared as melt intercalation method. Since the synthesis procedures for all the hybrids were very similar, only a representative example, the procedure for the preparation of the nanocomposite containing 2 wt% C_{12}PPh-MMT, is described here. 90.1 g of 1,4-butane diol (BD) (1.0 mole) and 2.24 g of C_{12}PPh-MMT were placed in a polymerization tube; the mixture was stirred for 30 min at room temperature. 97 g of dimethyl terephthalate (DMT) (0.5 mole) and 60 mg (2.1×10^{-4} mole) of isopropyl titanate were placed in a separate tube, and the organoclay/BD system was added to this mixture. Mechanical stirring was used to obtain a homogeneously dispersed system. This mixture was heated for 1 h at 190 °C under a steady stream of N_2 gas. The temperature of the reaction mixture was then raised to 230 °C and maintained there for 2 h under a steady stream of N_2 gas. During this period, continuous generation of methanol was observed. Finally, the mixture was heated for 2 h at 260 °C at a pressure of 1 Torr. The product was cooled to room temperature and repeatedly washed with water. It was dried under vacuum at 70 °C for 1 day to obtain the hybrid. The polymers are soluble in mixed solvents. Therefore, a mixed solvent phenol/1,1,2,2-tetrachloroethane (w/w = 50/50) was used in the measurement of solution viscosity. The solution viscosity numbers (see Table I) range from 0.80 to 0.95 for C_{12}PPh-MMT hybrids and 0.81 to 0.91 for C_{12}PPh-Mica hybrids.

We tried to synthesize PBT hybrids containing more than 2 wt% C_{12}PPh-MMT using the *in-situ* intercalation approach. However, repeated attempts to polymerize the 3 wt% C_{12}PPh-MMT/PBT hybrid all failed due to bubbles produced in the polymerization reactor during the transesterification of DMT and BD. The problem of how to produce high molecular weight polymer hybrids with high organoclay contents without the formation of bubbles remains unresolved.

Extrusion. In order to make thin sheet, the composites were pressed with 2,500 kg/cm^2 for 2-3 min at 235 °C on a hot press. The sheet of thickness ~0.5 mm were dried in a vacuum oven at 110 °C for 24 h and then extruded through

Table I. Thermal Properties of PBT Hybrid Fibers

Organoclay wt%	D.R.[a]	C_{12}PPh-MMT					C_{12}PPh-Mica				
		I.V.[b]	T_g °C	T_m °C	T_D^{ic} °C	wt_R^{600d} %	I.V.	T_g °C	T_m °C	T_D^{i} °C	wt_R^{600} %
0 (pure PBT)	1	0.85	27	222	371	1	0.91	27	222	366	1
1	1	0.95	36	227	377	6	0.89	33	223	371	2
2	1	0.80	37	227	375	10	0.83	32	222	373	3
	12		36	227	376	10					
	18		36	227	376	10					
3	1						0.81	33	223	374	7
	12							33	222	374	7
	18							34	223	374	7

[a]Draw ration. [b]Inherent viscosities were measured 30 °C by using 0.1 g/100 mL solutions in a phenol/1,1,2,2-tetrachloroethane (w/w = 50/50) mixture. [c]Initial weight-loss onset temperature. [d]Weight percent of residue at 600 °C.

the die of a capillary rheometer. The hot extrudates were stretched through the die of the capillary rheometer (INSTRON 5460) at 235 °C and immediately drawn at the constant speed of the take-up machine to form fibers with different DR. The pure PBT and PBT hybrids were each extruded into fibers with varying DR through a capillary die, and the thermal properties and the tensile mechanical properties of the extrudates were examined. The standard die diameter (DR = 1) was 0.75 mm. All the hybrid fibers obtained from the capillary rheometer were bright yellow. The DR was calculated from the ratio of the velocity of extrusion to the take up speed. The mean residence time in the capillary rheometer was ~3-4 min.

Characterization. The thermal behavior of the fibers was studied using a Du Pont model 910 differential scanning calorimeter (DSC) and thermogravimetric analyzer (TGA) at a heating rate of 20 °C/min under N_2 flow. Wide-angle X-ray diffraction (XRD) measurements were performed at room temperature using a Rigaku (D/Max-IIIB) X-ray diffractometer with Ni-filtered Cu-Kα radiation.

The tensile properties of the fibers were determined using an Instron mechanical tester (Model 5564) at a crosshead speed of 20 mm/min at room temperature. The experimental uncertainties in the ultimate strength and initial modulus were determined from more than 10 independent measurements: they were ± 1 MPa and ± 0.05 GPa, respectively.

The morphologies of the fractured surfaces of the extruded fibers were investigated using a Hitachi S-2400 scanning electron microscopy (SEM). An SPI sputter coater was used to sputter-coat the fractured surfaces with gold for enhanced conductivity. The samples were prepared for transmission electron microscopy (TEM) by putting PBT hybrid fibers into epoxy capsules and then curing the epoxy at 70 °C for 24 h in vacuum. The cured epoxies containing the PBT hybrids were then microtomed into 90 nm thick slices, and the each slice was deposited onto a mesh 200 copper net. TEM photographs of ultrathin sections of the polymer/organoclay hybrid samples were obtained on an Leo 912 OMEGA, Carl Zeiss, installed at KBSI, using an acceleration voltage of 120 kV. The particle sizes of morphology were measured by using scale bar in each microphotograph.

Results and Discussion

XRD. The XRDs of pure PBT, the organoclays, and the PBT/organoclay hybrid fibers are shown in Figures 1(a) and (b). The organic modified clays exhibit improved compatibility with polymers, so the clay galleries can easily be intercalated with the polymer. As expected, ion exchange between the Na^+-clays (Na^+-MMT and Na^+-Mica) and dodecyltriphenylphosphonium chloride ($C_{12}PPh\text{-}Cl^-$) was found to result in an increase in the basal interlayer spacing over that found in the pristine clays, and in a big shift of the

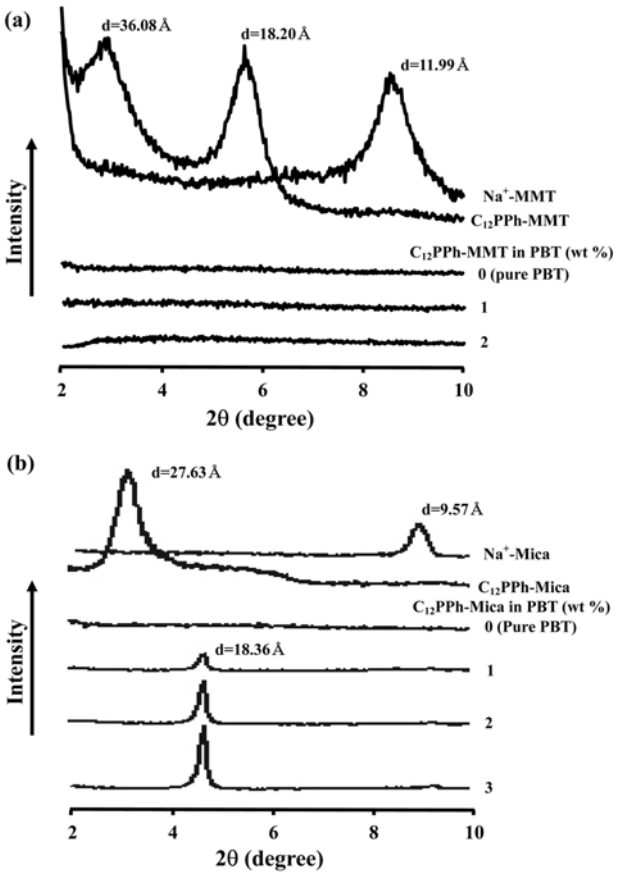

Figure 1. XRD patterns for clay, organoclay, and PBT hybrid fibers with various organoclay contents: (a) $C_{12}PPh$-MMT and (b) $C_{12}PPh$-Mica.

diffraction peak toward lower values of 2θ: the d spacing increased from 11.99 to 36.08 Å ($2\theta = 2.86°$) for $C_{12}PPh$-MMT and from 9.57 to 27.63 Å ($2\theta = 3.68°$) for $C_{12}PPh$-Mica. The interlayer spacing, d, of $C_{12}PPh$-MMT was found to be larger than that of $C_{12}PPh$-Mica. In general, an increase in the interlayer spacing should enhance the intercalation of the polymer chains, and lead to easier dissociation of the clay, which results in hybrids with better clay dispersion.[18-20] A second XRD peak in Figure 1(a) due to $C_{12}PPh$-MMT was also observed at $2\theta = 5.65°$ ($d = 18.20$ Å), which is associated with the (002) plane of the organoclay layers.

When the $C_{12}PPh$-MMT/PBT hybrid fibers form, the organoclay peak at $2\theta = 2.86°$ ($d = 36.08$ Å) disappears from the diffraction pattern (see Figure 1(a)). The structure of polymer nanocomposites is typically elucidated using XRD and TEM. Whereas XRD offers a convenienct way to determine the interlayer spacing due to the periodic arrangement of clay layers in the virgin clay and polymer nanocomposites,[21] TEM allows a qualitative understanding of the microstructure through direct visualization. XRD and TEM have been regarded as complementary in characterizing the mor-

phology of the polymer nanocomposites. Thus, the electron microscopy analyses provide the principal evidence in next section for the formation of the nanocomposites.

As shown in Figure 1(b), only a small peak at d = 18.36 Å (2θ = 4.81°) was found in the XRD results for the PBT extrudate fibers with 1 wt% C_{12}PPh-Mica content. This indicates that the mica layers of the organoclays were intercalated (not exfoliated) and not homogeneously dispersed in the PBT matrix. Substantial increases in the intensities of the XRD peaks were observed as the clay loading was increased from 1 to 3 wt%, suggesting that dispersion is more effective for lower clay loadings than for higher clay loadings. Higher clay loadings are expected to result in increased agglomeration of some portion of the clay within the PBT matrix. The disappearance of the main peaks for the PBT hybrid fibers (at 2θ = 2.86° for C_{12}PPh-MMT and at 2θ = 3.68° for C_{12}PPh-Mica) is thought to occur because the diffraction peaks due to the organoclay swollen with polymer chains are present at 2θ less than 2°.[18,20]

Figure 2 shows the XRD results for PBT hybrid fibers containing 2 wt% C_{12}PPh-clay for various values of DR. For increases in DR from 1 to 18, no obvious clay peaks appeared, as shown in Figure 2(a). Figure 2(b) also shows the XRD results for PBT hybrid fibers containing 2 wt% C_{12}PPh-Mica for various values of DR. For PBT with an organoclay content of 2 wt%, a peak is present at d = 18.36 Å (2θ = 4.81°) for DR = 1. In contrast to the results for the C_{12}PPh-MMT hybrids, substantial decreases in the XRD peak intensities were observed with increases in DR from 1 to 18, which suggest that an increase in DR should decrease the diameter and the clay content in hybrid fibers, and lead to decrease XRD peak.

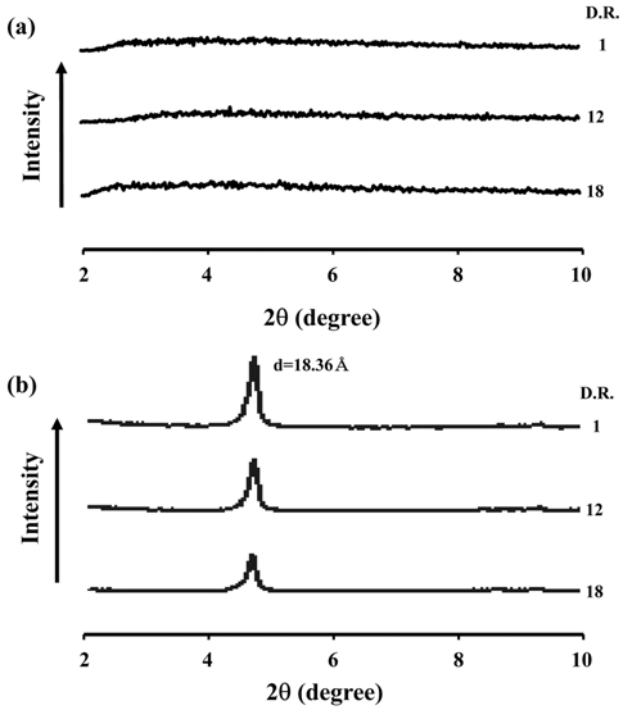

Figure 2. XRD patterns of 2 wt% organoclay in PBT hybrid fibers with different draw ratios: (a) C_{12}PPh-MMT and (b) C_{12}PPh-Mica.

Morphology. The SEM images of fractured surfaces of PBT hybrid fibers containing the two different organoclays are shown in Figures 3 to 6. The morphologies of the extruded fibers obtained from the PBT hybrid systems with various C_{12}PPh-MMT contents were determined by carrying out SEM examinations of their fracture surfaces, and the results are shown in Figure 3. Figure 3 shows the clay

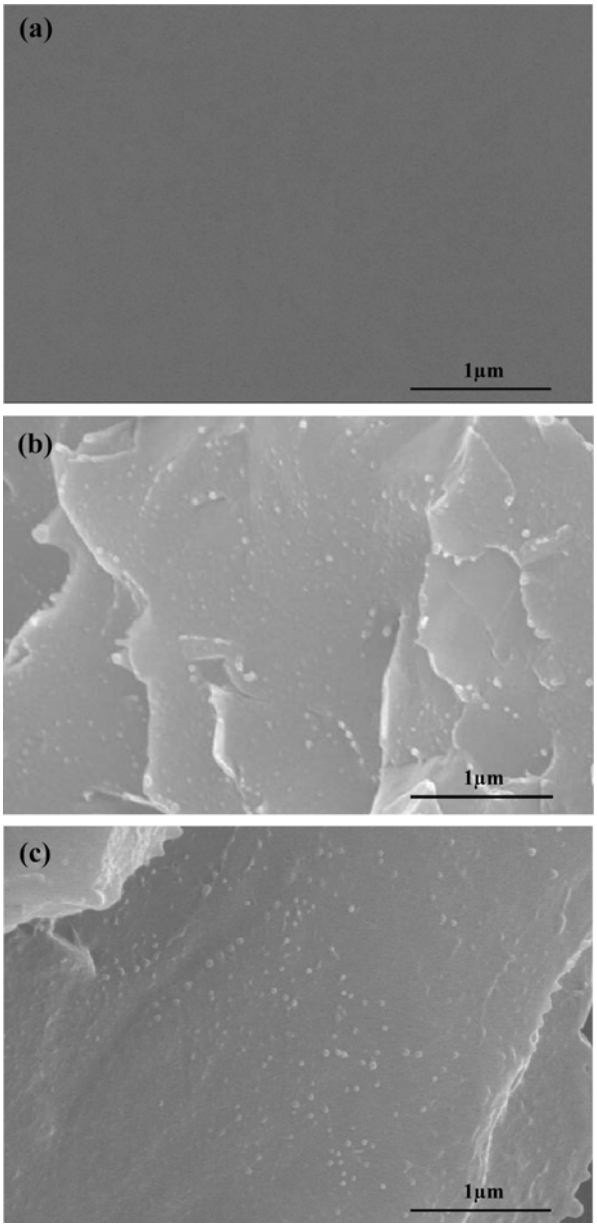

Figure 3. SEM photographs of (a) 0 (pure PBT), (b) 1, and (c) 2 wt% C_{12}PPh-MMT in PBT hybrid fibers.

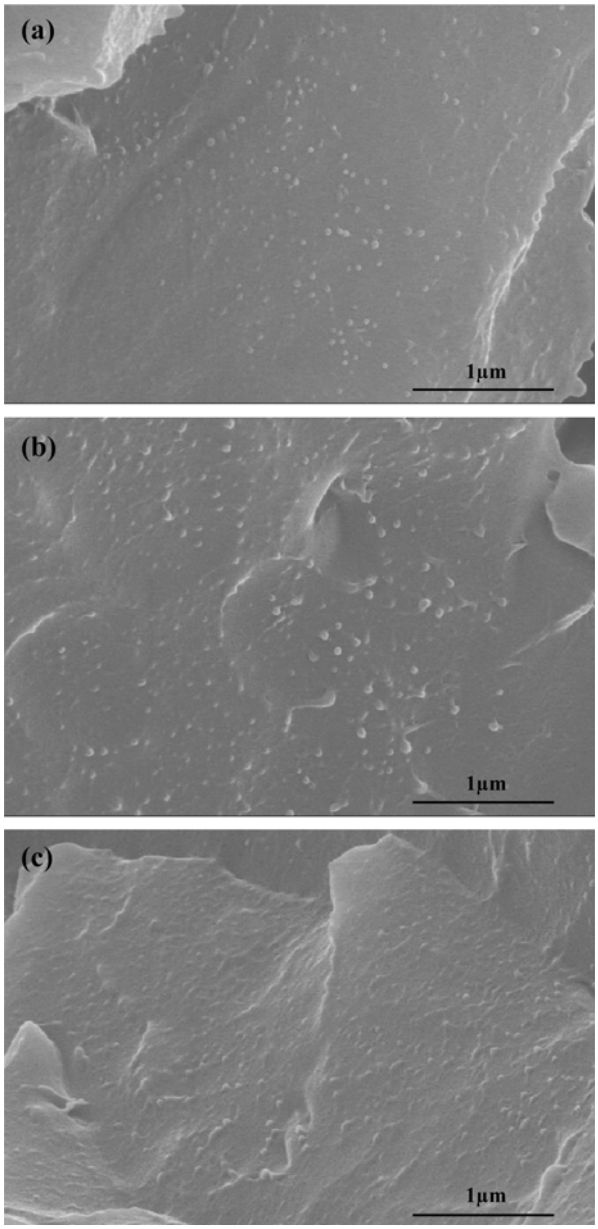

Figure 4. SEM photographs of 2 wt% C_{12}PPh-MMT in PBT hybrid fibers for draw ratios: (a) 1, (b) 12, and (c) 18.

phases that formed in undrawn hybrid fibers with organoclay contents ranging from 0 to 2 wt%. The PBT hybrid fibers with 0-2 wt% C_{12}PPh-MMT have morphologies consisting of clay domains, 80-100 nm in size, that are well dispersed in a continuous PBT phase. Figure 4 show micrographs of 2 wt% C_{12}PPh-MMT/PBT hybrid fibers obtained at DRs ranging from 1 to 18. The 2 wt% hybrid fiber with DR = 12 contains fine clay phases 60-110 nm in diameter (see Figure 4(b)). The hybrid fiber with DR = 18 also exhibits fine dispersion with domains 30-50 nm in diameter (see Figure 4(c)). The domain size of the dispersed clay phase was found to decrease linearly with increasing DR. The fine dis-

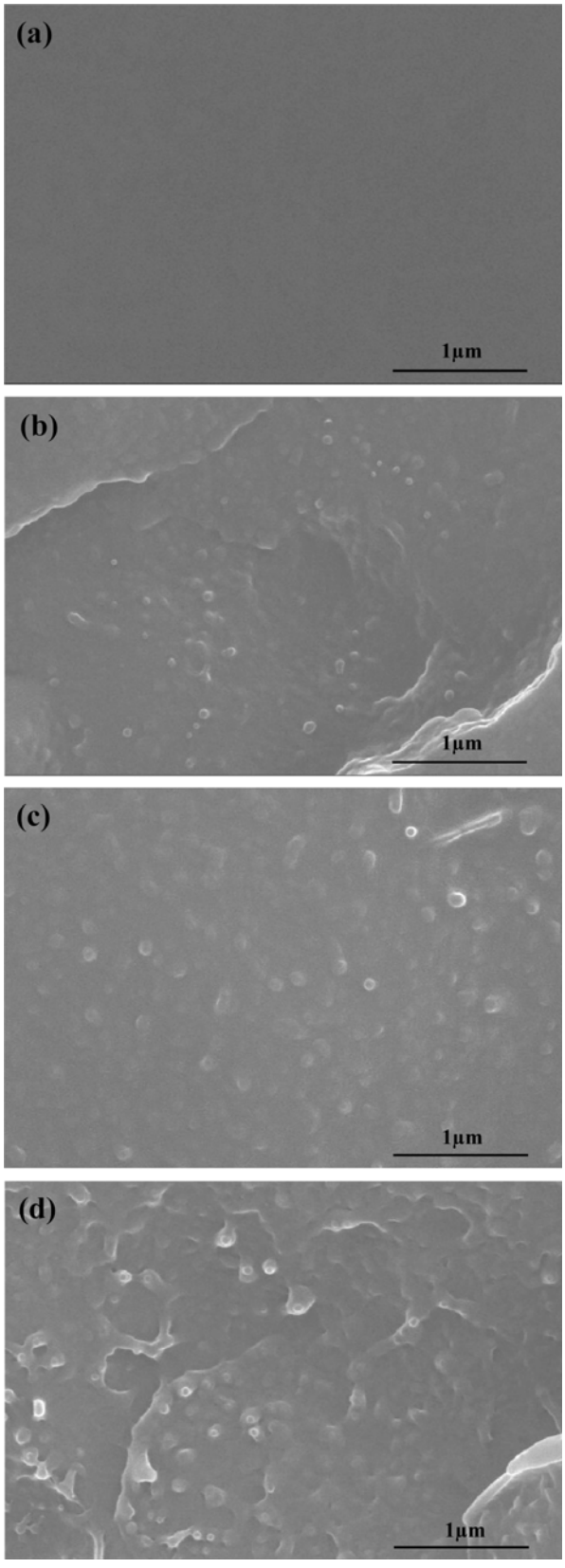

Figure 5. SEM photographs of (a) 0 (pure PBT), (b) 1, (c) 2, and (d) 3 wt% C_{12}PPh-Mica in PBT hybrid fibers.

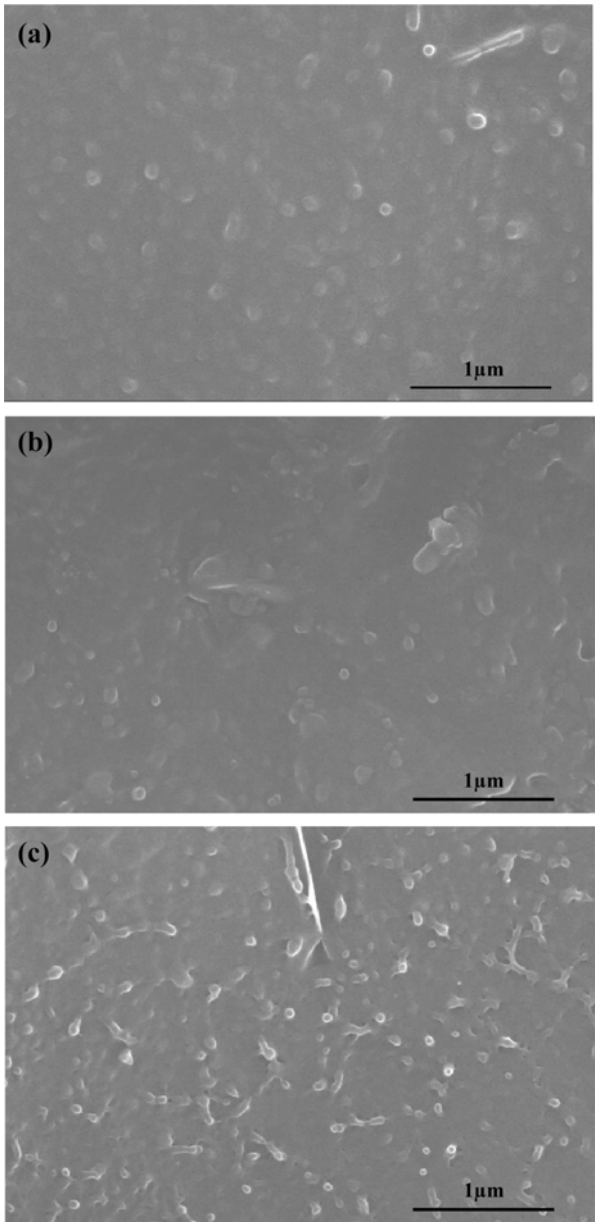

Figure 6. SEM photographs of 2 wt% C_{12}PPh-Mica in PBT hybrid fibers for draw ratios: (a) 1, (b) 12, and (c) 18.

persion of the clay seems to be the result of the stretching of the fiber that occurs when the extrudates pass through the capillary rheometer.

The PBT hybrid fibers with 0-3 wt% C_{12}PPh-Mica for DR = 1 have morphologies consisting of clay domains that are 100-250 nm in particle diameter (see Figure 5). Figure 6 shows micrographs of 2 wt% C_{12}PPh-Mica/PBT hybrid fibers obtained for various DRs in the range 1 to 18. The 2 wt% hybrid fiber with DR = 12 contains fine clay phases that are 100-200 nm in diameter (see Figure 6(b)). The hybrid fiber with DR = 18 also contains pull-out particles with domain sizes of 100-150 nm (see Figure 6(c)). The average clay particle size was found to decrease slightly with increasing DR, which is consistent with the XRD results in Figure 2(b).

To examine exactly the dispersion of the clay layers in the fiber hybrids, we carried out TEM studies. A TEM allows a qualitative understanding of the internal structure through direct observation. More direct evidence of the formation of true nanocomposites is provided by our TEM micrographs of the ultramicrotomed sections. The TEM micrographs in Figures 7 and 8 show the structures of the fibers, at DR = 1, for different magnifications. The dark lines are the intersections of the 1 nm thick sheet layers. Increasing the magnification in an area occupied by an aggregate reveals that the individual sheets of MMT clay are separated by a layer of polymer, as can be seen in Figure 7(b). Thus the morphology consists of a mix of intercalated and exfoliated sheets,

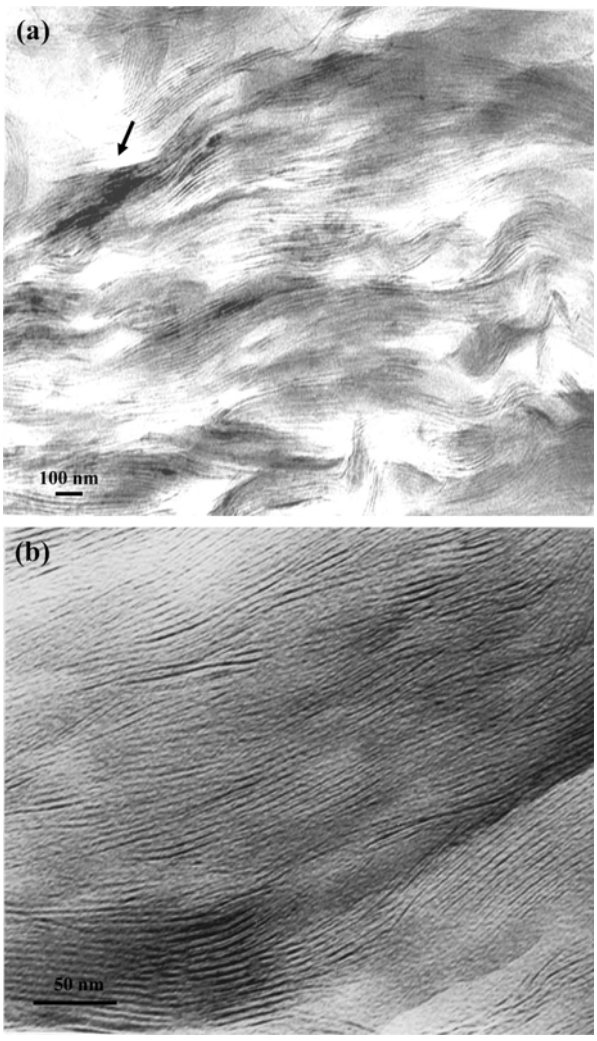

Figure 7. TEM photographs of 2 wt% C_{12}PPh-MMT in PBT hybrid fibers (DR = 1) increasing the magnification levels from (a) to (b).

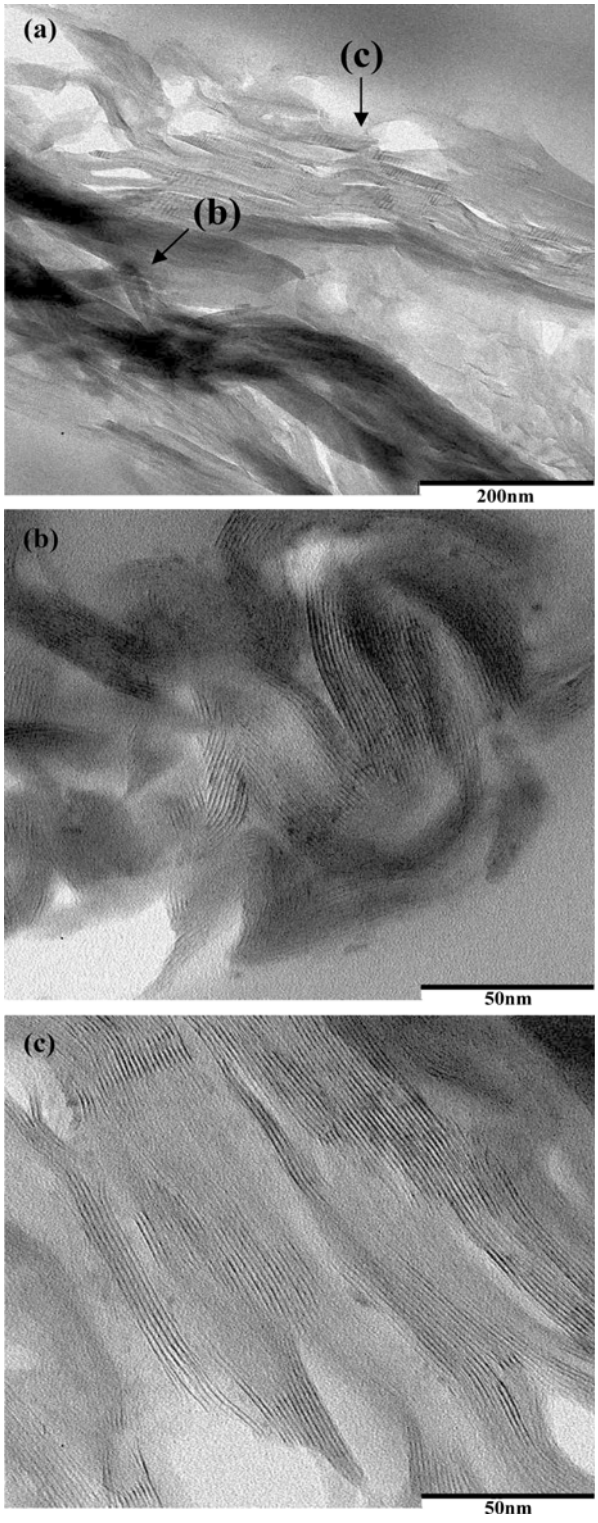

Figure 8. TEM photographs of 2 wt% C_{12}PPh-Mica in PBT hybrid fibers (DR = 1) increasing the magnification levels from (a) to (c).

i.e., there are regions where a regular stacking arrangement is maintained with a layer of polymer between the sheets, and also regions where completely delaminated sheets are dispersed individually. Figure 8 shows TEM photographs of 2 wt% C_{12}PPh-Mica/PBT hybrid fibers, in which the organoclay can be seen to be well dispersed in the polymer matrix at all magnification levels, although some of the clay particles are agglomerated at size levels greater than approximately 20 nm. The peaks in the XRD patterns of these samples are attributed to these agglomerated layers (see Figure 1(b)). Compared to the hybrids containing C_{12}PPh-Mica, the clay layers of the C_{12}PPh-MMT hybrid fibers (Figures 1(a), 2(a), and 7) are more exfoliated within the matrix polymer.

Figures 7 and 8 also show that the clay layers are dispersed homogeneously within the matrix polymer, which indicates that nanocomposites have been formed, although some clusters or agglomerated particles were also detected. Therefore clays such as MMT and Mica are broken down via *in situ* intercalative polymerization into nano-scale building blocks and dispersed homogeneously in polymer matrices to afford polymer/clay nanocomposites. The unusual thermo-mechanical properties of these nanocomposites are discussed in the following sections, and are attributed to the homogeneous dispersion of the silicate nano-scale particles.

Thermal Behaviors. The thermal properties of pure PBT and of PBT/organoclay hybrids with various DRs are listed in Table I. The glass transition temperatures (T_g), melting transition temperatures (T_m), and initial decomposition temperatures at 2% weight loss (T_D^i) of the hybrids increase with increases in C_{12}PPh-MMT content up to 1 wt%, and then remain constant with further increases in the organoclay loading. For example, the T_g, T_m, and T_D^i of C_{12}PPh-MMT/PBT hybrid fibers with 1 wt% clay loading are higher by 9, 5, and 6 °C, respectively, than those of pure PBT, and are not significantly different for 2 wt% clay content. Similarly, the T_g and T_D^i of C_{12}PPh-Mica hybrid fibers with 1 wt% clay loading are higher by 6 and 5 °C, respectively, than those of pure PBT, and do not vary significantly up to 3 wt% clay content.

The observed increases shown in Table I in the glass transition temperatures of these hybrids with the addition of the organoclay could be the result of several different factors,[8] in particular the increase in cross-link density and the restriction of the segmental relaxation of the chain segments near the clay layers. Similar results have been obtained in other studies of polymer nanocomposites.[22,23] The increase in T_m with the addition of organoclay may result from the heat insulating effects of the clay layer structure, as well as from the interactions between the organoclay and the PBT molecular chains.[24] The presence of the clay also enhances the initial decomposition temperatures by acting as an insulator and as a mass-transport barrier to the volatile products generated during decomposition.[25-27] This increase in the thermal stability can also be attributed to the high thermal stability of the clay and to the interactions between the clay

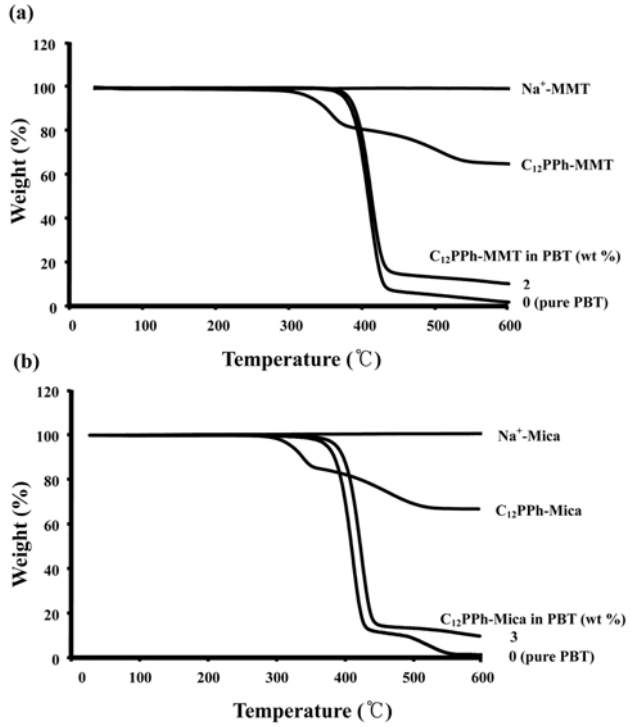

Figure 9. TGA thermograms of clay, organoclay, and PBT hybrid fibers with various organoclay contents: (a) C_{12}PPh-MMT and (b) C_{12}PPh-Mica.

particles and the polymer matrix. The TGA curves for the clay, the organoclay, and PBT hybrid fibers with various organoclay contents are shown in Figure 9.

In contrast to the thermal properties, the weight of the residue at 600 °C was found to increase monotonically with increases in the clay loading, as shown in Table I. This enhancement of char formation with increasing organoclay content is ascribed to the high heat resistance of the clay.[28] In Table I, it can be seen that the thermal properties of the PBT hybrid fibers with the two different organoclays are virtually unchanged with increases in DR from 1 to 16.

Mechanical Tensile Properties. Pure PBT and the PBT hybrids were extruded through a capillary die with various DRs to determine the tensile strengths and moduli of the extrudates. The tensile mechanical properties of PBT and its hybrids are given in Table II. It can be seen that the ultimate strengths of the C_{12}PPh-MMT hybrids increase gradually with increasing organoclay content and are highest for a clay content of 2 wt% and DR = 1. The ultimate tensile strength of 2 wt% PBT hybrid fibers is 58 MPa, which is about 41% higher than that of pure PBT (41 MPa). The ultimate tensile strength of the C_{12}PPh-Mica hybrid fibers at DR = 1 increases with the addition of clay up to a critical clay loading, and then decreases above that critical content. For example, the strengths of the hybrids were found to increase from 41 to 50 MPa with an increase in the organoclay content to 2 wt%. This improvement arises because the organoclay layers are dispersed and intercalated in the PBT matrix. This result is consistent with the general observation that the introduction of an organoclay into a matrix polymer increases its tensile strength.[29-31] When the amount of organo-mica in PBT reaches 3 wt%, the strength decreases to 47 MPa. This decrease in ultimate strength is mainly due to the agglomeration of clay particles above the critical clay loading, as we have previously reported.[32,33]

The modulus values were found to increase linearly with increasing organoclay content. When the C_{12}PPh-MMT content was increased to 2 wt%, the modulus of the hybrid was found to be 3.33 GPa, about 2.5 times as great as that of pure PBT (1.37 GPa). The initial modulus values of the

Table II. Tensile Properties of PBT Hybrid Fibers

Organoclay wt%	D.R.[a]	C_{12}PPh-MMT			C_{12}PPh-Mica		
		Ult. Str. (MPa)	Ini. Mod. (GPa)	E.B.[b] (%)	Ult. Str. (MPa)	Ini. Mod. (GPa)	E.B.[b] (%)
0 (pure PBT)	1	41	1.37	3	41	1.37	3
	12	43	1.69	3	43	1.69	3
	18	46	1.71	3	46	1.77	3
1	1	55	2.96	3	48	2.21	4
	12	52	2.57	3	44	2.25	3
	18	48	2.33	2	42	2.28	3
2	1	58	3.33	2	50	2.61	3
	12	35	2.45	2	41	2.62	2
	18	28	2.21	2	41	2.67	2
3	1				47	2.80	3
	12				45	2.80	2
	18				44	2.87	2

[a]Draw ratio. [b]Elongation percent at break.

C_{12}PPh-Mica hybrid fibers were also found to increase significantly with increases in the organoclay content. For an organoclay content of 3 wt%, the modulus of the hybrid was found to be 2.80 GPa, about 2.0 times that of pure PBT (1.37 GPa). This increased initial modulus could be the result of two different factors: the high resistance of the clay, and the orientation and the aspect ratio of the clay layers. Further, increasing the clay content increases the constraints on polymer chain mobility, which also increases the modulus.[34,35]

The increases in the tensile strength and the initial modulus of pure PBT with increases in DR were found to be insignificant. For pure PBT, the strength and the modulus were found to increase from 41 to 46 MPa and 1.37 to 1.71 GPa, respectively, as the draw ratio was increased from 1 to 18, as shown in Table II. Unlike flexible coil-like polymers, the values of the ultimate strength and the initial modulus of the hybrid fibers were found to decrease markedly with increasing DR, as shown in Table II. For hybrid fibers with 1 wt% C_{12}PPh-MMT, their tensile strength and the initial modulus decreased from 55 to 48 MPa and from 2.96 to 2.33 GPa, respectively, as DR was increased from 1 to 18. Similar trends were observed for hybrid fibers with 2 wt% C_{12}PPh-MMT.

A similar result was observed for the C_{12}PPh-Mica hybrid fibers. For example, for hybrid fibers with an organoclay content of 1 wt%, increases in DR from 1 to 18 resulted in decreases in the tensile strength from 48 to 42 MPa. Similar trends were observed for hybrid fibers with organoclay contents of 2 and 3 wt%. An increase in the tensile strength with increases in DR is very common for engineering plastics and is also usually observed for flexible coil-like polymers. However, our system did not follow this trend. The observed decline in the tensile properties seems to be due to debonding between the organoclay and the matrix polymer, and to the presence of the many nano-sized voids that result from excess stretching of the fibers. This indicates that hydrostatic elongation during the extrusion and compression molding operations results in debonding in the polymer chain as well as in void formation around the polymer-clay interfaces.[36,37]

In contrast to the decreases in the lower tensile strength

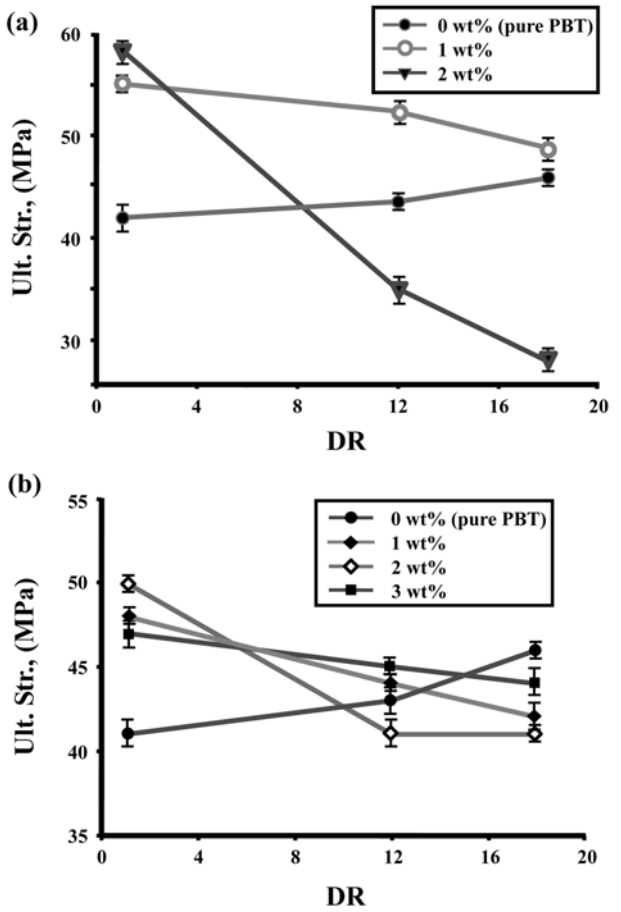

Figure 10. Effects of draw ratio on the ultimate tensile strength of various organoclay contents in PBT hybrid fibers: (a) C_{12}PPh-MMT and (b) C_{12}PPh-Mica.

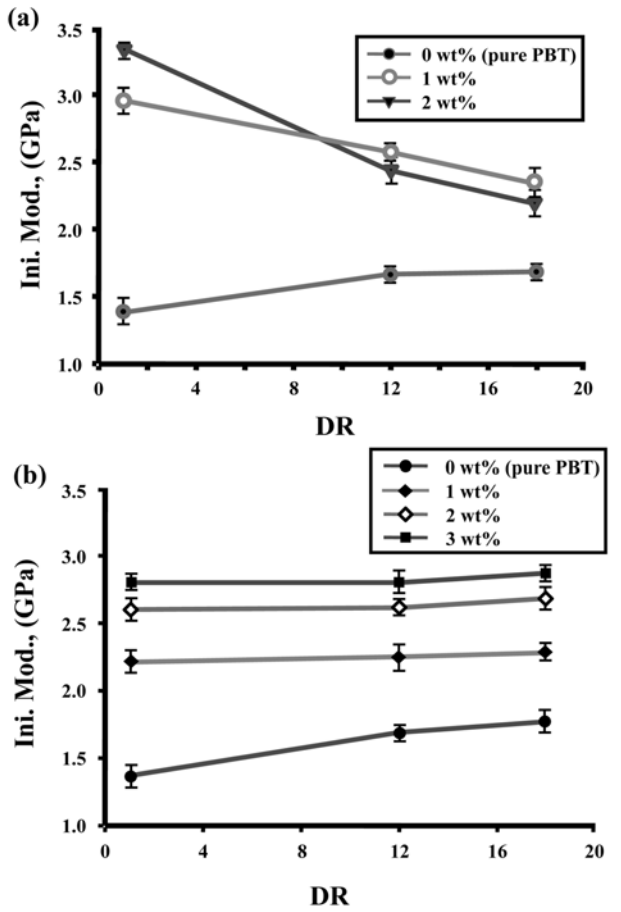

Figure 11. Effects of draw ratio on the initial tensile modulus of various organoclay contents in PBT hybrid fibers : (a) C_{12}PPh-MMT and (b) C_{12}PPh-Mica.

values, the initial moduli of the C_{12}PPh-Mica hybrid fibers were found to increase slightly with increases in DR for a given clay content, as shown in Table II. This enhancement of the modulus is ascribed to the high resistance of the clay. The stretching resistance of the oriented backbones of the polymer chains in the gallery also contributes to the enhancement of the modulus. The variations in the ultimate strengths and initial moduli of the PBT hybrid fibers are plotted against clay content for varying DR in Figures 10 and 11 respectively.

The elongation at breakage of the C_{12}PPh-MMT and C_{12}PPh-Mica hybrids was found to be virtually unchanged with variation in DR, i.e. it was found to increase from 2 to 4% as DR was increased from 1 to 18. This result is characteristic of materials reinforced with stiff inorganic materials, and is indicative of intercalated morphology.

Conclusions

Considerable effort has been expended in the attempt to improve the thermo-mechanical properties of common thermoplastics by blending them with organoclays. In this investigation, we tried to clarify the structural effects of the phosphonium-type organoclay reinforcement of the PBT matrix in fiber form. The dispersions of the organoclays with PBT were synthesized by using the *in-situ* intercalation method for various organoclay contents to produce nanoscale composites. Some clay layers were found to be dispersed homogeneously in the matrix polymer, although some clusters were also detected.

The thermal properties (T_g, T_m, and T_D^i) of the hybrid fibers were found to be better than those of pure PBT fibers. However, these thermal properties remained unchanged for DRs ranging from 1 to 18. The tensile properties of the hybrid fibers were found to increase gradually with increasing C_{12}PPh-MMT content at DR = 1. However, the ultimate strengths and initial moduli of the hybrid fibers decreased markedly with increasing DR. Further, the addition of only a small amount of organoclay was found to be sufficient to improve the tensile mechanical properties of the C_{12}PPh-Mica/PBT hybrid fibers. In this work, the properties of C_{12}PPh-MMT/PBT hybrids were found to be better than those of C_{12}PPh-Mica/PBT hybrids.

References

(1) A. Nogales, G. Broza, Z. Roslaniec, K. Schulte, I. Syics, and B. S. Hsiao, *Macromolecules*, **37**, 7669 (2004).
(2) D. Wu, C. Zhou, W. Yu, and X. Fan, *J. Polym. Sci.; Part B: Polym. Phys.*, **43**, 2807 (2005).
(3) J.-H. Chang and R. J. Farris, *Polym. J.*, **27**, 780 (1995).
(4) J. M. Park and Y. H. Park, *Macromol. Res.*, **13**, 128 (2005).
(5) J. Y. Kim, S. W. Kang, and S. H. Kim, *Macromol. Res.*, **13**, 19 (2005).
(6) G. Lagaly, *Appl. Clay. Sci.*, **15**, 1 (1999).
(7) A. Usuki, A. Koiwai, Y. Kojima, M. Kawasumi, A. Okada, T. Kurauchi, and O. Kamigaito, *J. Appl. Polym. Sci.*, **5**, 119 (1995).
(8) K. Yano, A. Usuki, A. Okada, T. Kurauchi, and O. Kamigaito, *J. Polym. Sci.; Part A: Polym. Chem.*, **31**, 2493 (1993).
(9) E. P. Giannelis, *Adv. Mater.*, **8**, 29 (1996).
(10) J.-H. Chang, B. S. Seo, and D. H. Hwang, *Polymer*, **43**, 2969 (2002).
(11) K. Yano, A. Usuki, and A. Okada, *J. Polym. Sci.; Part A: Polym. Chem.*, **35**, 2289 (1997).
(12) J. M. Garcia-Martinez, O. Laguna, S. Areso, and E. P. Collar *J. Polym. Sci.; Part B: Polym. Phys.*, **38**, 1564 (2000).
(13) S. H. Hwang, S. W. Paeng, J. Y. Kim, and W. Huh, *Polym. Bull.*, **49**, 329 (2003).
(14) D. Wang, J. Zhu, Q. Yao, and C. A. Wilkie, *Chem. Mater.*, **14**, 3837 (2002).
(15) P. C. LeBaron, Z. Wang, and T. J. Pinnavaia, *Appl. Clay Sci.*, **12**, 11 (1999).
(16) J.-H. Chang, S. J. Kim, and S. Im, *Polymer*, **45**, 5171 (2004).
(17) J.-H. Chang and M. K. Mun, *J. Appl. Polym. Sci.*, **100**, 1247 (2006).
(18) S. H. Hsiao, G.. S. Liou, and L. M. Chang, *J. Appl. Polym. Sci.*, **80**, 2067 (2001).
(19) C. Zilig, R. Mulhaupt, and J. Finter, *Macromol. Chem. Phys.*, **200,** 661 (1999).
(20) Y. Ke, J. Lu, X. Yi, X, Zhao, and Z. Qi, *J. Appl. Polym. Sci.*, **78**, 808 (2000).
(21) C. H. Davis, L. J. Mathias, J. W. Gilman, D. A. Schiraldi, J. R. Shields, P. Trulove, T. E. Sutto, and H. C. Delong, *J. Polym. Sci.; Part B: Polym. Phys.*, **40**, 2661 (2002).
(22) F. Li, J. Ge, P. Honigfort, S. Fang, J. C. Chen, F. Harris, and S. Cheng, *Polymer*, **40**, 4987 (1999).
(23) A. Agag and T. Takeichi, *Polymer*, **41**, 7083 (2000).
(24) M. Hussain, R. J. Varley, Z. Mathys, Y. B. Cheng, and G. P. Simon, *J. Appl. Polym. Sci.*, **91**, 1233 (2004).
(25) T. D. Fornes, P. J. Yoon, D. L. Hunter, H. Keskkula, and D. R. Paul, *Polymer*, **43**, 5915 (2002).
(26) H. R. Fischer, L. H. Gielgens, and T. P. M. Koster, *Acta. Polym.*, **50**, 122 (1999).
(27) X. S. Petrovic, L. Javni, A. Waddong, and G. J. Banhegyi, *J. Appl. Polym. Sci.*, **76**, 133 (2000).
(28) J. Wen and G. L. Wikes, *Chem. Mater.*, **8**, 1667 (1996).
(29) T. Lan and T. J. Pinnavaia, *Chem. Mater.*, **6**, 2216 (1994).
(30) K. Masenelli-Varlot, E. Reynaud, G. Vigier, and J. Varlet, *J. Polym. Sci.; Part B: Polym. Phys.*, **40**, 272 (2004).
(31) J. W. Cho and D. R. Paul, *Polymer*, **42**, 1083 (2001).
(32) J.-H. Chang, M. K. Mun, and I. C. Lee, *J. Appl. Polym. Sci.*, **98**, 2009 (2005).
(33) M.-K. Mun, J. C. Kim, and J.-H. Chang, *Polym. Bull.*, **57**, 797 (2006).
(34) L. Chen, S. C. Wong, and S. J. Pisharath, *J. Appl. Polym. Sci.*, **88**, 3298 (2003).
(35) Y. Kojima, A. Usuki, M. Kawasumi, A. Okada, Y. Fukushima, T. Kurauchi, and O. Kamigaito, *J. Mater. Res.*, **8**, 1185 (1993).
(36) W. A. Curtin, *J. Am. Ceram. Soc.*, **74**, 2837 (1991).
(37) D. Shia, Y. Hui, S. D. Burnside, and E. P. Giannelis, *Polym. Eng. Sci.*, **27**, 887 (1987).